

Effects of variability of local winds on cross ventilation for a simplified building within a full-scale asymmetric array:

Gough, H.; Sato, T.; Halios, C.; Grimmond, C. S. B.; Luo, Z.; Barlow, J. F.; Robertson, A.; Hoxey, R.; Quinn, A.

DOI:

[10.1016/j.jweia.2018.02.010](https://doi.org/10.1016/j.jweia.2018.02.010)

License:

Creative Commons: Attribution (CC BY)

Document Version

Publisher's PDF, also known as Version of record

Citation for published version (Harvard):

Gough, H, Sato, T, Halios, C, Grimmond, CSB, Luo, Z, Barlow, JF, Robertson, A, Hoxey, R & Quinn, A 2018, 'Effects of variability of local winds on cross ventilation for a simplified building within a full-scale asymmetric array: Overview of the Silsoe field campaign', *Journal of Wind Engineering and Industrial Aerodynamics*, vol. 175, pp. 408-418. <https://doi.org/10.1016/j.jweia.2018.02.010>

[Link to publication on Research at Birmingham portal](#)

General rights

Unless a licence is specified above, all rights (including copyright and moral rights) in this document are retained by the authors and/or the copyright holders. The express permission of the copyright holder must be obtained for any use of this material other than for purposes permitted by law.

- Users may freely distribute the URL that is used to identify this publication.
- Users may download and/or print one copy of the publication from the University of Birmingham research portal for the purpose of private study or non-commercial research.
- User may use extracts from the document in line with the concept of 'fair dealing' under the Copyright, Designs and Patents Act 1988 (?)
- Users may not further distribute the material nor use it for the purposes of commercial gain.

Where a licence is displayed above, please note the terms and conditions of the licence govern your use of this document.

When citing, please reference the published version.

Take down policy

While the University of Birmingham exercises care and attention in making items available there are rare occasions when an item has been uploaded in error or has been deemed to be commercially or otherwise sensitive.

If you believe that this is the case for this document, please contact UBIRA@lists.bham.ac.uk providing details and we will remove access to the work immediately and investigate.



Effects of variability of local winds on cross ventilation for a simplified building within a full-scale asymmetric array: Overview of the Silsoe field campaign

H. Gough^{a,*}, T. Sato^b, C. Halios^a, C.S.B. Grimmond^a, Z. Luo^c, J.F. Barlow^a, A. Robertson^d, R. Hoxey^d, A. Quinn^d

^a Department of Meteorology, University of Reading, United Kingdom

^b Department of Energy and Environmental Engineering, IGSES Kyushu University, Japan

^c School of the Built Environment, University of Reading, United Kingdom

^d School of Civil Engineering, University of Birmingham, B15 2TT, United Kingdom

ABSTRACT

The large body of natural ventilation research, rarely addresses the effects of the urban area on ventilation rates. A novel contribution to this gap is made by the REFRESH cube campaign (RCC). During 9 months of observations, the Silsoe cube was both isolated and surrounded by a limited asymmetrical staggered array. A wide range of variables were measured continuously, including: local, reference and internal flow, stability, background meteorological conditions, internal temperature, and ventilation rates (pressure difference techniques for cross ventilated cases). This paper tests the impact of the array on the relation between local and reference wind speeds as modified by wind direction and on cross ventilation rates. The presence of the array causes a 50%–90% reduction in normalised ventilation rate when the reference wind direction is normal to the cube. The decrease in natural ventilation varies with wind direction with large amounts of scatter for both setups. The relation between local and reference wind speeds for the array case had two characteristic responses, not explained by reference wind (speed or direction) nor sensitive to averaging period, turbulence intensity or temperature differences. Given the singular response of the CIBSE approach, it is unable to capture these conditions.

1. Introduction

A building with insufficient ventilation may experience excessive condensation, overheating and a build-up of pollutants (Hens et al., 1996), affecting occupant health and comfort. Occupants report a somewhat higher degree of satisfaction with the indoor environment when naturally ventilated, despite higher temperatures and the possibility of higher levels of CO₂ compared to mechanically ventilated buildings (Hummelgaard et al., 2007). As natural ventilation uses wind pressure and buoyancy to replace internal air with external air to maintain indoor air quality and thermal comfort (Short et al., 2004) it is considered an environmentally sustainable ventilation method (Allocca et al., 2003).

Natural ventilation is difficult to predict within an urban area due to variations in building form, orientation, local meteorological conditions and complex urban structures. The urban environment creates challenges for the application of natural ventilation within it: lower wind speeds, variable wind directions, elevated noise and pollution levels and higher temperatures due to the urban heat island effect. Yuan and Ng (2012) and Cheng et al. (2012) highlighted that the increased urbanisation in Hong

Kong has led to wind stagnation and blockage. Changes in local wind direction due to the influence of buildings have added more difficulty in predicting ventilation rate of buildings (Jiang and Chen, 2002). Reductions in natural ventilation rates between an isolated building and an urban area can vary between 33% (CIBSE, Chartered Institute for Building Service Engineers, 2006) and 96% (van Hooff and Blocken, 2010). The potential for daytime natural ventilation is reduced within an urban canyon (Santamouris et al., 2001). Their conclusions are drawn from simulations informed by measurements of 10 canyons in Athens with both single sided and cross ventilated buildings (window 1.5 × 1.5 m). Airflow was reduced up to 5 (single-sided) and 10 (cross-ventilation) times, due to changes in wind direction and wind speed within the canyon (Santamouris et al., 2001).

For investigation, the complexity and individuality of urban environments is often simplified either in street layout or building form, removing details such as the presence of small architectural features, foliage and structures (e.g. bridges, street furniture). Urban areas are often treated as arrays of rectangular buildings described by morphological parameters, including building size and spacing (Kanda, 2007; Barlow and Coceal, 2009). These simplifications make basic flow

* Corresponding author. University of Reading, Department of Meteorology, Earley Gate, PO Box 243, Reading RG6 6BB, United Kingdom.
E-mail address: h.gough@reading.ac.uk (H. Gough).

mechanisms more obvious and are often used to parameterize urban boundary layer processes in numerical weather prediction models (Grimmond et al., 2010). For example, flow at street intersections is highly dependent on the surrounding morphology (Dobre et al., 2005).

Often cuboid scale models are used to represent buildings in the wind tunnel (Cheng et al., 2007; Zaki et al., 2010; Hall and Spanton, 2012); the field, such as the array of 512 1.5 m cubes (Comprehensive outdoor scale model, COSMO, Inagaki and Kanda, 2010) and the UMIST Environmental Technology centre test site, 1:10 scale cube array (Macdonald et al., 1998); and in computational fluid dynamics (CFD) modelling (Coceal et al., 2007). Some sites are studied using more than one approach; for example, the COSMO site has been investigated in the wind tunnel (Sato et al., 2010) and using CFD (Inagaki et al., 2012), and similarly the Mock Urban Setting Test (MUST) (Gailis and Hill, 2006) and UMIST (Macdonald et al., 1998) sites. In the real-world array studies (e.g. COSMO, MUST, UMIST) a focus was having true external flow conditions. However, in none of these were there measurements of ventilation rates of the buildings or a combined focus of internal and external flow conditions.

Full-scale measurements capture the variability of a site's atmospheric conditions (stability, turbulence, wind direction, wind speeds, temperature), but at the expense of experimental repeatability. All scales of turbulence are captured, some of which may not be accurately modelled by wind tunnel and CFD models (Richards and Hoxey, 2007). Full-scale ventilation studies of specific building types include work in hospitals (Gilkeson et al., 2013), schools (Bakó-Biró and Clements-Croome, 2012) and supermarkets (Kolokotroni et al., 2015) are often limited by flow characterisation. In the wind tunnel, flows must have physically realistic boundary layer velocity profiles and turbulence characteristics as these influence the flow patterns around the building model. Full-scale measurements of wind characteristics around a building array to which wind tunnel or modelling work can be compared are very rare (Richards and Hoxey, 2007).

Internal building flows depend, in part, on the external flows. The relation between external and internal flow is a growing area of research, with little known about buildings experiencing highly turbulent urban flows. This is relevant to how to design appropriate ventilation strategies (Liddament, 1996) which is frustrated in part due to the small amount of full-scale building data available (Blocken, 2014). However, some studies have compared coupled internal and external flow measurements with scale models (e.g. Karava et al., 2011) and CFD (e.g. King et al., 2017).

The specific focus of this paper is testing the impact of the array on the i) relation between local and reference wind speeds as modified by wind direction and ii) cross ventilation rates. The CIBSE recommendations are assessed. This paper presents an overview of the full-scale measurements undertaken within RCC – REFRESH cube campaign. The RCC is the first to explore flow characteristics and ventilation, in and around, a full-scale building surrounded by a limited array of cubes.

2. Methodology

The full-scale field campaign RCC – REFRESH cube campaign involved extensive data collection (Gough, 2017). In this study of natural ventilation, both the urban environment and the low-rise building investigated are simplified. The building, a 6 m × 6 m × 6 m metal cube (Richards and Hoxey, 2002, 2008), was located in rural Silsoe, UK. Previously, it has been used to explore surface pressure trends (Richards et al., 2001; Richards and Hoxey, 2012, 2012a) and ventilation (Straw et al., 2000; Yang et al., 2006) amongst other topics. Thus, the site is well-characterised. Additionally, it has been modelled in the wind tunnel (Richards and Hoxey, 2007) and by CFD (Yang et al., 2006).

The cube's removable panels (0.4 m wide and 1 m high, centre point 3.5 m) permit it to be sealed or single sided or cross ventilated (Straw et al., 2000). In this study it is reduced from 1 m² to lower flow rates. The cube faced into the prevailing wind direction (approximately 240°), hereafter this is referred to as 0°, with clockwise angles being positive and anticlockwise angles being negative (Fig. 1). Therefore, 0° denotes

flow perpendicular to the front opening of the cube (Front or West face: Fig. 2) with ±90° being parallel to the openings.

Although no topographic features were close enough to the site to have an effect, the surroundings were not uniform. The site had a road to the east and agricultural fields with crop stumps (~0.1 m high) to the west. There is good exposure to winds from South-West (~15°) to East (180°) with a surface roughness length of 0.006–0.01 m (Richards and Hoxey, 2012). Local structures include two storage tanks (~2 m high and 4 m wide, black triangle, Fig. 1) and a storage shed (15 m wide and 25 m long with a sloping roof, black diamond, Fig. 1) with roughly the same height as the instrumented cube.

The urban environment for RCC was created from eight straw cubes (equivalent dimensions to the metal cube) arranged in a staggered asymmetrical pattern around the metal cube. With a total area of 1260 m², this leads to a plan area density (building: total surface area, λ_p) of 25.7% (Fig. 1). Straw was chosen as it could withstand prolonged exposure to strong winds and met the site owner's specified constraints. Although the sides and tops of the cubes were not completely smooth at this high Reynolds number, the form drag of the cube is assumed to dominate the flow and pressure patterns rather than the viscous drag of the cubes.

RCC observations were undertaken in two spatial arrangements: the array (Fig. 1) was in place October 2014 to April 2015, and the cube was isolated from May 2015 to July 2015. All instruments had the same set-up for whole period to allow for clear comparisons. All data reported here are averaged over 30 min periods (unless otherwise stated) so it would capture all significant contributions to flow variability due to atmospheric boundary layer turbulence (Kaimal and Finnigan, 1993).

2.1. Instrumentation

During the full-scale RCC observations, seven 3-axis Gill R3-50 sonic anemometers, measuring three-component wind velocity and direction, were deployed: two within the cube itself and five outside (Fig. 1). The two sonic anemometers closest to the instrumented cube (Front and Back, Fig. 1) and two internal sonic anemometers were mounted on masts, with the centre of the sonic anemometer at 3.5 m above ground level (in line with the opening centre). All sonic anemometers were positioned at the same height to study flow into and out of the cube. The Channel mast (Fig. 1) sonic anemometer was at 2.9 m (maximum height for the equipment) and logged at 20 Hz. All others were logged simultaneously at 10 Hz to a MOXA UC 7410 Plus fan-less compact computer. Post processing of the data followed the methodology of Barlow et al. (2014) and Wood et al. (2010). The sonic anemometers were inter-compared before and after the experiment. As no drift and minimal differences were observed, no inter-instrument corrections are made.

The cube surface pressure was measured using pressure taps: 7 mm holes located centrally on 0.6 m² steel panels, which were mounted flush onto the cube cladding to minimise their effect on the pressures measured (Fig. 2). Pressure signals were transmitted pneumatically, using 6 mm internal diameter plastic tubes to transducers within the cube. The individual transducers meant that the pressure tap measurements were simultaneous at 10 Hz. The pressure differential sensors for pressure taps 1–16 (Fig. 2) were Honeywell 163PC01D75 differential pressure sensors with a range of –2.5–2.5 inches of H₂O (~–498–498 Pa). Pressure taps 17–32 (Fig. 2) were Honeywell 163PC01D76 differential pressure sensors with a range of –5 to 5 inches of H₂O (~–1245–1245 Pa). All pressure sensors had a manufacturer stated response time of 1 ms.

30 external pressure taps and 2 internal pressure taps were used. The internal pressure measurements were located under the openings in the same position as used in Straw (2000) as internal pressures may vary over time. The 30 external pressure taps used were split across the four faces, four on the roof, four in a horizontal array on the centre line across the North and South faces and nine on the front and back faces, with five of those in a vertical array down the centre and four in a horizontal array at

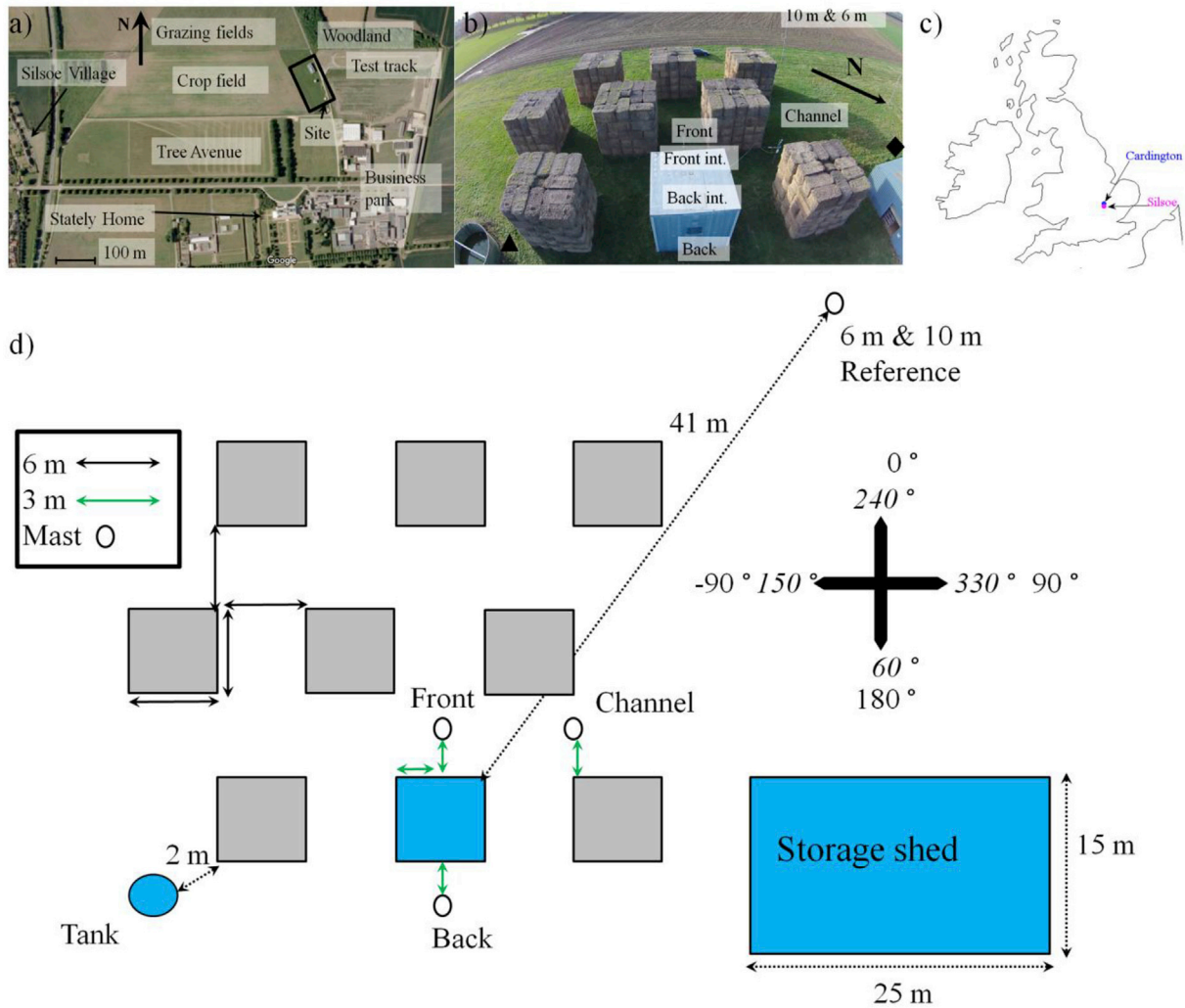


Fig. 1. RCC full-scale study site at Silsoe: a) plan view with the main features (unchanged since 2009), b) oblique view into the prevailing wind direction of the cube array, with sonic anemometer locations, storage shed (black diamond) and sewage tanks (black triangle), c) location of Silsoe, U.K., and the Met Office Cardington site, U.K., d) plan of the site with angle notation. The blue cube in (b) and square in (d) is the instrumented cube. All cubes are 6 m by 6 m by 6 m. Sources of a: Copyright 2016 Infoterra, Blue Sky Limited and Google Earth. (For interpretation of the references to colour in this figure legend, the reader is referred to the Web version of this article.)

half building height (Fig. 2). The taps on the North and South faces are not centred due to pre-existing tapping points (Straw et al., 2000) being used and the limited reach of the pipes.

A reference pressure was measured using a static pressure probe (in house, Richards and Hoxey, 2012), with a reference dynamic pressure measured using a directional pitot tube (in house) at 6 m (building height) alongside the 6 m reference sonic anemometer (Fig. 1).

On the channel mast (Fig. 1), external temperature, atmospheric pressure and rainfall were measured by a Vaisala WXT520 weather station, a Kipp and Zonen CNR4 net radiometer measured the four components of radiation (data used to indicate day/night periods) and an open path LI-COR LI-7500 CO₂ and H₂O gas analyser provided CO₂ and H₂O concentrations at station pressure.

2.2. Cross ventilation rate

The surface pressure measurements were undertaken continuously, providing a large dataset with visible trends. The ventilation rate (Q) derived from the measured façade wind pressure difference was calculated using the standard orifice equation:

$$Q = C_d A \sqrt{\frac{2\Delta p}{\rho_0}} \quad (1)$$

where Δp is the pressure difference between the internal and external environments, ρ_0 is the density of the flow, A is the opening area and C_d is the discharge coefficient (measured to be $0.61 \pm 5\%$ for these openings through wind tunnel testing of a full-scale model window). The external pressure was deduced from the average of the taps surrounding the window (i.e. taps 12, 26, 27, 11 for the Back face). Q is calculated assuming the flow is approximately turbulent under normal pressures. The error for each ventilation rate is the total from all variables (eqn. (1)) measurement errors. Although uncertainty (varying with conditions) arises from 30-min ventilation calculations rather than using the instantaneous values (Choinière et al., 1992), given 30-min averaging is required for the meteorological data, it is deemed appropriate for ventilation calculations.

3. Results

Observations were taken across a wide range of meteorological

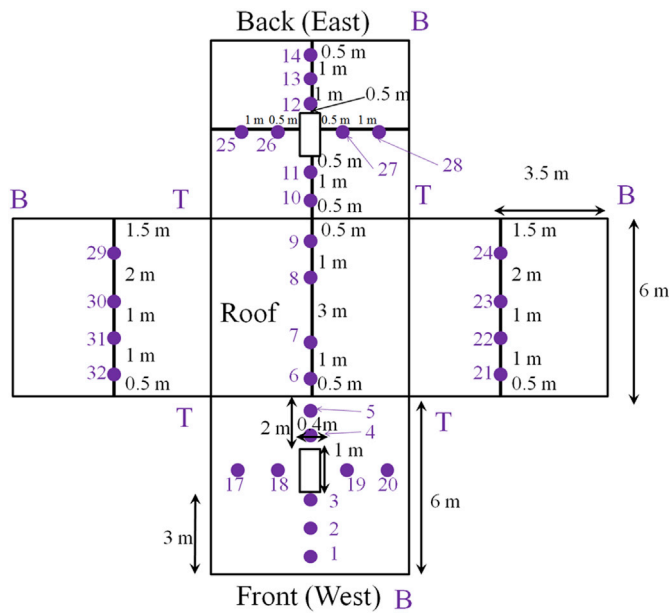


Fig. 2. Location of the pressure taps on each face (T top, B base) of the cube with distance between taps (black) and the opening (white rectangles). Internal taps 15 and 16 are not shown. (drawing not to scale). The front and back faces are symmetrical as are the side faces.

conditions (Fig. 3, Table 1) with the prevailing wind direction south-westerly for both the isolated and array cases (Fig. 3). Despite the relatively long duration of study, not all wind directions were captured for the isolated cube and array cases (Fig. 3). The reference flow measurements taken at 6 m and 10 m upstream of the array on the same mast showed good agreement with measurements at the closest UK Met Office station in Cardington (~15 km N) for wind speed and direction (Fig. 1). The site maximum 30-min mean wind speed at 6 m was 13.1 m s^{-1} , both this and the minimum wind speed occurred during the array observation period (Fig. 3). The maximum turbulence intensity is associated with the minimum reference wind speed (U_{ref}) for the array case (Table 1). For the isolated cube, the high turbulence intensities occurred when the reference wind direction (θ_{ref}) was approximately 60° , suggesting that the storage shed may have impacted the reference wind speed measurements (Fig. 1). The isolated case experienced higher external temperatures

(Table 1), likely caused by the array shading the instrument (Fig. 1, channel mast). There were periods where all or some of the instruments were offline due to malfunctions or power cuts: these are removed from the final count in Table 1.

3.1. Flow within the array

Reference wind speeds are often used to predict the local flow within an urban environment and thus the ventilation rate of a building. However, as the urban environment is complex the reference flow may not be representative of the local wind speed and direction. In this section the relation between the reference and local wind speeds for the RCC dataset are explored, to determine if predictable patterns can be identified therefore permitting more accurate wind speed, and thus ventilation rates, estimation.

In this study the front mast (Fig. 1) is treated as the representative of the local flow which impacts on the instrumented cube and drives ventilation. The front mast is referred to as the local mast. Although for cross ventilation for certain wind directions, the back mast may be more representative of the local driving flow, these wind directions are rare (Fig. 3) and the mast itself is on the edge of the array, with no obstacles either side, so it does not experience flow determined by the array.

Fig. 4 shows that when 30-min wind speed averages from the 6 m (reference) and the front (local, 3.5 m) masts are compared, three distinct clusters of points or “behaviours” (a, b and c) can be quantitatively defined by the ratio of U_{local} to U_{ref} : a occurs for ratios greater than 0.4, b for ratios between 0.15 and 0.4 and c occurs for ratios under 0.15. These thresholds were determined by splitting the data into three categories and iterating the threshold values until the R^2 values for a linear regression of U_{local} against U_{ref} for each category (a, b or c) were maximised. Whilst there are trends with wind direction, it is difficult to draw solid conclusions. For example, behaviour a, where the local windspeed is highest, occurs for some periods when $\theta_{ref} = \pm 180^\circ$, where the reference flow is impacting on the back of the instrumented cube. Behaviour a also encompasses wind directions of $\theta_{ref} = \pm 90^\circ$, where flow is parallel to the array and travels along the streets.

Behaviours b and c occur for overlapping θ_{ref} values and both behaviours occur when θ_{ref} is limited to $\pm 10^\circ$ from perpendicular across all averaging periods from 1 to 60 min (not shown), suggesting they are not an artefact of the chosen averaging period. The behaviours in Fig. 4 were found to be unrelated to internal-external temperature difference, standard deviation of the reference wind direction, turbulence intensity of

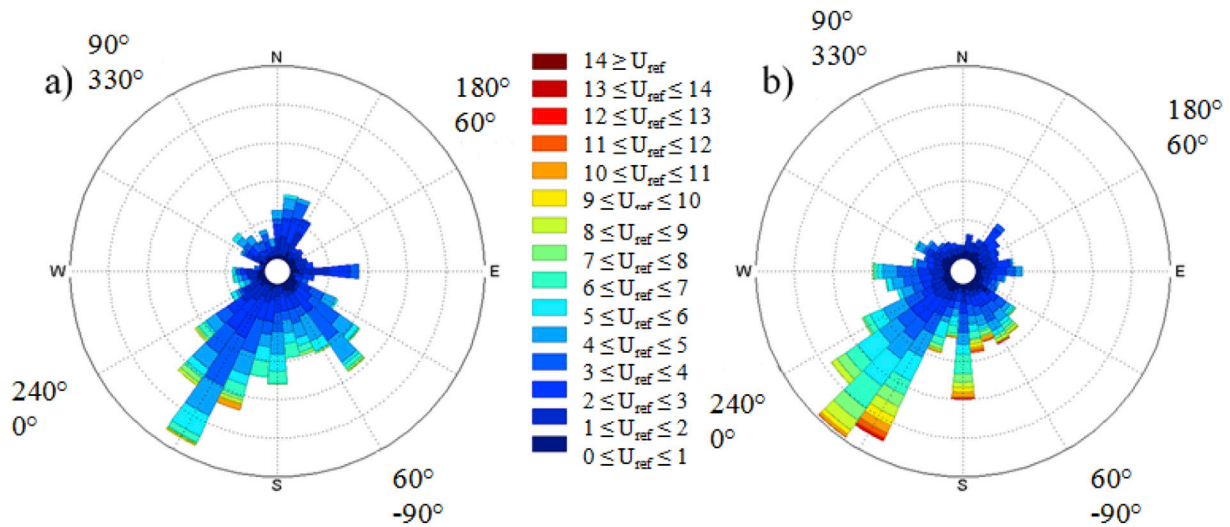


Fig. 3. Wind roses for 30-min means for the a) isolated cube and b) array periods of RCC (Table 1). U_{ref} (colour) is taken at 6 m with frequency of θ_{ref} being shown by bar length. The prevailing south-westerly winds are evident. Inner labels are meteorological θ_{ref} values, outer labels are with respect to the cube (Fig. 1). (For interpretation of the references to colour in this figure legend, the reader is referred to the Web version of this article.)

Table 1
Range of conditions measured during the RCC field campaign for the isolated and array cases: number of 30-min averages (N), reference wind speed (U_{ref}), reference wind direction (θ_{ref}), atmospheric stability, turbulence intensity, σ_u/U_{ref} (TI) (where σ_u is the standard deviation of the u wind component) at 6 m and external air temperature (2.9 m, Fig. 1). The wind components have been rotated into the mean wind direction following the methodology outlined in Wilczak et al. (2001) and Wood et al. (2010). Stability is defined as z/L where z is measurement height and L is Obukhov length obtained from the 6 m mast (assuming displacement height is negligible). Standard error is given for each.

| Set-up | N | Range | | | | |
|-------------------------------|------|--------------------------------|--------------------|---------------------|----------------|-------------------------|
| Period (DD/MM/YY) | | U_{ref} (m s ⁻¹) | θ_{ref} (°) | Stability (z/L) | TI | External T_{air} (°C) |
| Isolated 30/05/15–07/07/15 | 1712 | 0.04–10.10 ± 0.02 | 0–359 ± 1 | –15–15 ± 0.1 | 0.13–3 ± 0.05 | 5.1–33.8 ± 1.0 |
| Array 09/10/14–30/04/15 | 6102 | 0.01–13.1 ± 0.02 | 0–359 ± 1 | –10–10 ± 0.1 | 0.05–15 ± 0.05 | –2.4–21.4 ± 1.0 |

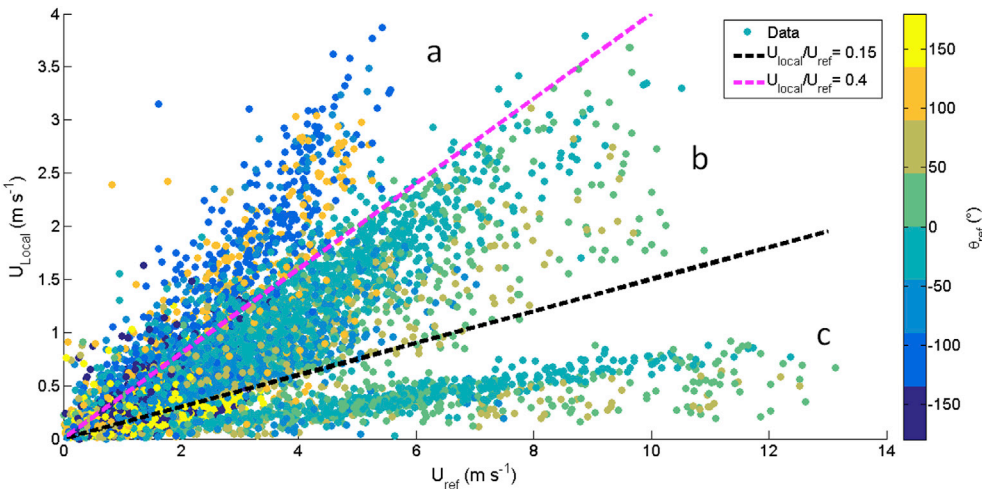


Fig. 4. Wind speeds (30-min averages) measured when the RCC array was present at the local (U_{local}) and 6 m reference (U_{ref}) masts with direction indicated by colour bar as measured at the reference (θ_{ref}) mast. Three distinct behaviours are labelled and the value of U_{local}/U_{ref} used to separate the behaviours is shown (dashed lines). Wind speed errors are $\sim 2\%$ of the measurement. Wind direction has a 1° error. (For interpretation of the references to colour in this figure legend, the reader is referred to the Web version of this article.)

the reference wind, ventilation set up, atmospheric stability or reference wind speed. The number of 30-min periods in each regime (**b** and **c**) is approximately equal (2260 and 2085, respectively).
To further explore the three behaviours, the relation between θ_{ref} and θ_{local} are investigated with the behaviour colour coded (Fig. 5). For a θ_{ref}

the local flow can be in multiple directions. For example, for $-60 < \theta_{ref} < +70^\circ$, behaviours **b** and **c** have different trends in θ_{local} values. For behaviour **b**, θ_{local} remains within 10° – 40° , representing channelled flow from the west through the array. However, for behaviour **c**, θ_{local} is reversed compared to θ_{ref} , suggesting that the local mast is

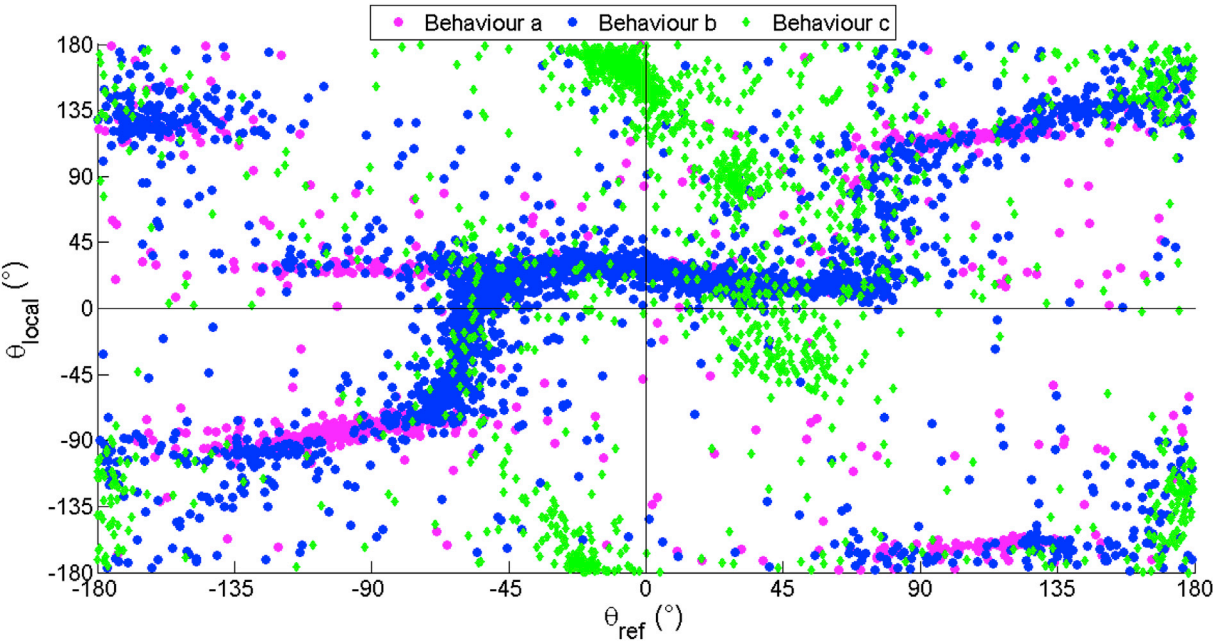


Fig. 5. Local (θ_{local}) and reference (θ_{ref}) wind directions colour coded for the three behaviours identified in Fig. 4. (For interpretation of the references to colour in this figure legend, the reader is referred to the Web version of this article.)

caught in the recirculation region of upstream buildings. There is dual behaviour for almost all θ_{ref} values, suggesting the flow within the array can be in differing states at a single location depending on θ_{ref} .

The pattern in Fig. 5 is similar to a comparison of local and reference wind speeds for an urban intersection in the DAPPLE project (Barlow et al. (2009)). Horizontal trends suggest flow is being channelled (e.g. $-135^\circ < \theta_{ref} < -60^\circ$ where θ_{local} is approximately -90° or -30°) whereas vertical trends (e.g. $70^\circ < \theta_{ref} < 90^\circ$) indicate where the local mast is being influenced by a highly unsteady wake or potentially, is being influenced by interacting wakes. Oblique trends (e.g. behaviour **c** for $-45^\circ < \theta_{ref} < 45^\circ$) suggests wake reflection, where there are low wind speeds present (Fig. 4). Behaviour **a**, where local windspeeds are highest, corresponds mostly to channelling flow, whereas lower wind speed behaviours **b** and **c** coincide with both wakes and channel flows.

Flow features interacting may also result in flow which is converging (channelling effects) or diverging (wake effects) within the canopy (Boddy et al., 2005; Nelson et al., 2007). This result suggests that a building array could be split into streets, where the flow is being channelled and intersections, where flow is likely to have intermittent features such as recirculating wakes (Dobre et al., 2005). The split behaviour seen in this study is dependent on θ_{ref} , therefore knowledge of the relative orientation of a building to the prevailing wind direction could help determine which “regime” is likely for most of the time and thus if wind speeds are moderate or low.

Although some meteorological datasets are freely available for certain sites in the UK (e.g. London Heathrow, Edinburgh), these data may not be applicable for a given site due to distance or a change in terrain. CIBSE (2006) suggest a correction for wind speeds to use these non-local data sets:

$$U_z = U_R k z^a \quad (2)$$

where U_z is the wind speed at the desired location at height z , U_R is the wind speed at the meteorological mast (10 m in this case) and k and a are coefficients which depend on the surrounding terrain (Table 2). It is important to note that this is a generic equation, which does not account

Table 2
Terrain coefficients (k , a) used in Eq. (2) (CIBSE, 2006).

| Terrain | k | a |
|------------------------------------|------|------|
| Open, flat country | 0.68 | 0.17 |
| Country with scattered wind breaks | 0.52 | 0.20 |
| Urban | 0.35 | 0.25 |
| City | 0.21 | 0.33 |

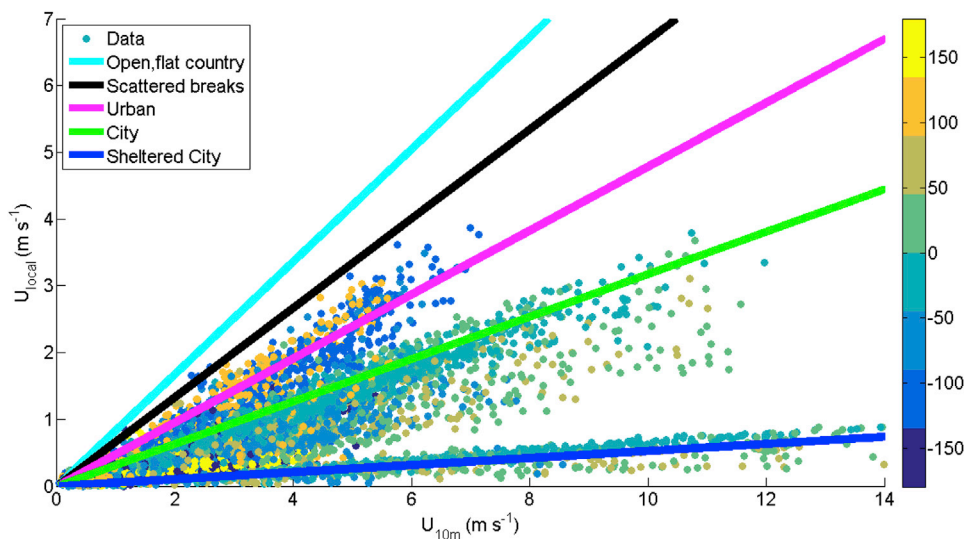


Fig. 6. Array wind speeds measured on the local (U_{local}) and reference (U_{ref}) masts and reference wind direction (colour). Coloured lines indicate Eq. (2) computed using the four CIBSE (2006) coefficients (Table 2) applied at 10 m as recommended and fitted to behaviour **c** data (“Sheltered City”). Errors as for Fig. 4. (For interpretation of the references to colour in this figure legend, the reader is referred to the Web version of this article.)

for specific site features or prevailing meteorology. The ability of this equation to provide representative local wind speeds is evaluated with the Silsoe array measurements.

The CIBSE wind speed predictions are shown with the observed data in Fig. 6. Whilst Eq. (2) cannot predict the split in behaviour, the “urban” coefficients provide a good fit to the linear trend within behaviour **a** and the “city” coefficients fit the linear trend within behaviour **b** reasonably well. However, the CIBSE predictions do not encompass behaviour **c** data at all. The “Sheltered City” coefficients ($k = 0.03$, $a = 0.45$) of Eq. (2) fits the behaviour **c** data (Fig. 6 blue). From Figs. 5 and 3 it is evident that the prevailing wind direction is $-30 \pm 15^\circ$, for which “wake dominant” behaviours **b** and **c** are most common. The direction-weighted average of $U_{loc}/U_{10m} = 0.30$, compared to the CIBSE “urban” value of 0.48 and “city” value of 0.32. This also indicates that the exposure of the Silsoe building in the array to prevailing winds is relatively sheltered, despite the limited extent of the array.

3.2. Cross ventilated natural ventilation variability with wind direction

To remove the bias of wind speed, all ventilation rates (Q) are normalised (Q_N):

$$Q_N = \frac{Q}{U_{ref} A} \quad (3)$$

by the opening area (A) and U_{ref} . A variety of normalised ventilation rates occurred when the cube was cross ventilated based on 30-min averaged data (Fig. 7). Cases (~ 30) with large internal and external temperature differences were removed. Cross ventilation is assumed to be entirely wind driven.

The ~ 100 tracer gas experiments undertaken did not sample all wind directions, therefore the relation between tracer gas decay ventilation rate and wind direction could not be determined for both the isolated and array set-ups. Thus, the pressure-based ventilation data set is used. With very large openings (‘large’ is undefined) the uncertainty of the pressure difference method increases because of the non-uniform distribution of the pressure differences and the velocity profile across the ventilation opening varying with time (Ogink et al., 2013).

For the isolated cube, the distribution of normalised ventilation rate (Q_N) is unsymmetrical (Fig. 7), unlike expectations from models (CIBSE, 1997). This is likely caused by the storage shed (Fig. 1) when $\theta_{ref} = 90^\circ$ and potentially the tanks when $\theta_{ref} = -90^\circ$ (Fig. 1). The woodland would also have an effect for $\theta_{ref} = 90^\circ$ to 130° (Fig. 1). The low Q_N values ($Q_N < 0.2$) for $\theta_{ref} = 0^\circ \pm 30^\circ$ is the result of low surface pressure

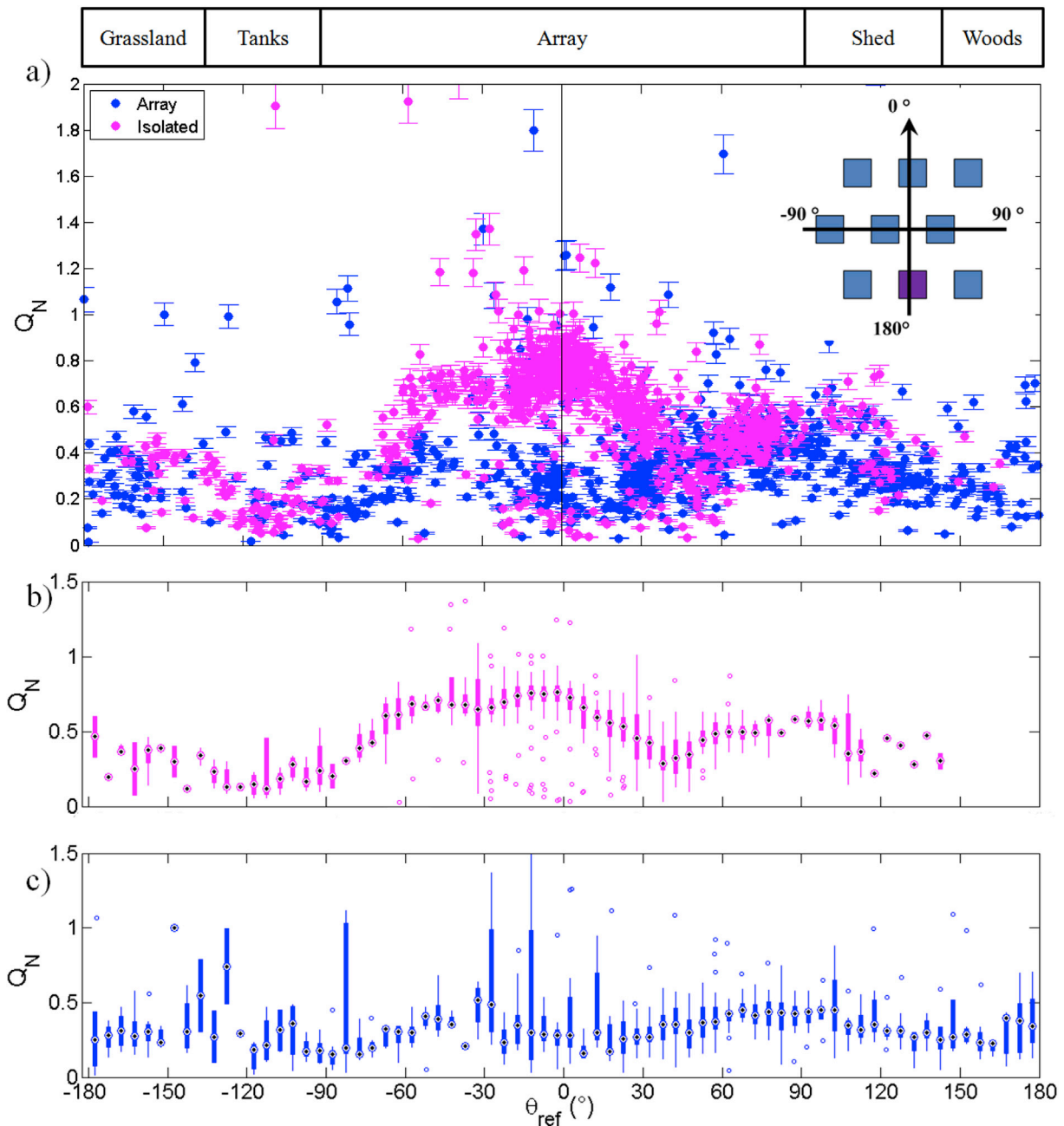


Fig. 7. Pressure derived 30-min averaged normalised ventilation rate (Q_N) for a cross ventilated building: a) all values with standard error bars; and box plots in 5° bins of b) isolated, c) array results. Box plots show the inter-quartile range (IQR), median (point), 1.5 times the IQR (whiskers), and outliers (points).

measurements but their cause is currently unknown.

Q_N is similar for the isolated and array cases when the flow is parallel to the array streets $\theta_{ref} = \pm 90^\circ$ and when the flow approaches from the back of the array ($\theta_{ref} = 135^\circ$ – 180° and $\theta_{ref} = -135^\circ$ – 180°) (Fig. 7) as the back of the instrumented cube is exposed (Fig. 1). For $\theta_{ref} = \pm 90^\circ$ variation of the wind direction within the 30-min average for the array case causes slight variations between the isolated and array cases (Fig. 7). Flow is also similar when $\theta_{ref} = 45^\circ$ – 60° but not for the equivalent negative angles, this is likely due to the arrays asymmetry with less shielding being present on the positive side, meaning some flow directly impacts the instrumented cube.

Sheltering by the array impacts the instrumented cube Q_N in an asymmetrical manner with respect to the θ_{ref} (Fig. 7). Maximum blockage occurs at $\theta_{ref} = 0^\circ$, when Q_N is approximately halved compared to the Q_N for the isolated cube. The array causes a 50%–90% reduction in

ventilation rate when $\theta_{ref} = 0^\circ$. The array case has more scatter with wind direction, probably related to the transient nature of the complex flow features occurring within the array (Fig. 6).

For both the isolated and array cases there are outliers from the general trend (Fig. 7). These are not linked to internal-external temperature differences or instrument malfunction. However, there can be variations of up to $1.2 Q_N$ (for $\theta_{ref} = 0^\circ$), suggesting that the wind driven ventilation increases for short periods of time, dependent on external conditions. Some of this variation can be explained by the split behaviour in wind speeds for $\theta_{ref} = 0^\circ$ (Fig. 8). For $U_{ref} < 2 \text{ m s}^{-1}$ all three behaviours result in similar U_{local} magnitudes. However, as U_{ref} increases differences occur, with trend a resulting in greater U_{local} speeds than behaviours b and c (Fig. 4). Behaviour c causes the lowest U_{local} magnitudes for $U_{ref} > 2 \text{ m s}^{-1}$ leading to the lowest ventilation rates for $\theta_{ref} = 0^\circ$ with outliers being when behaviours a and b occur (Fig. 8). The

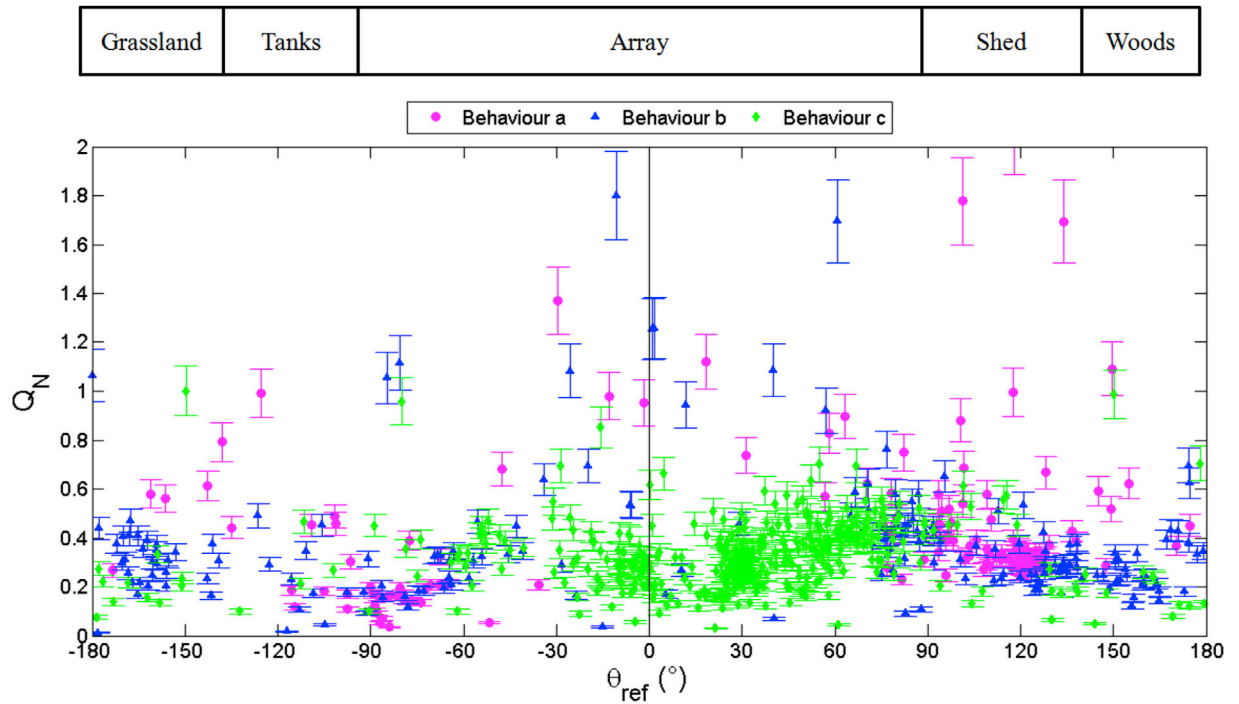


Fig. 8. Normalised ventilation rates for the array case (30-min average), stratified by the behaviours in Fig. 4 (colour). Errors are the same as Fig. 7a. (For interpretation of the references to colour in this figure legend, the reader is referred to the Web version of this article.)

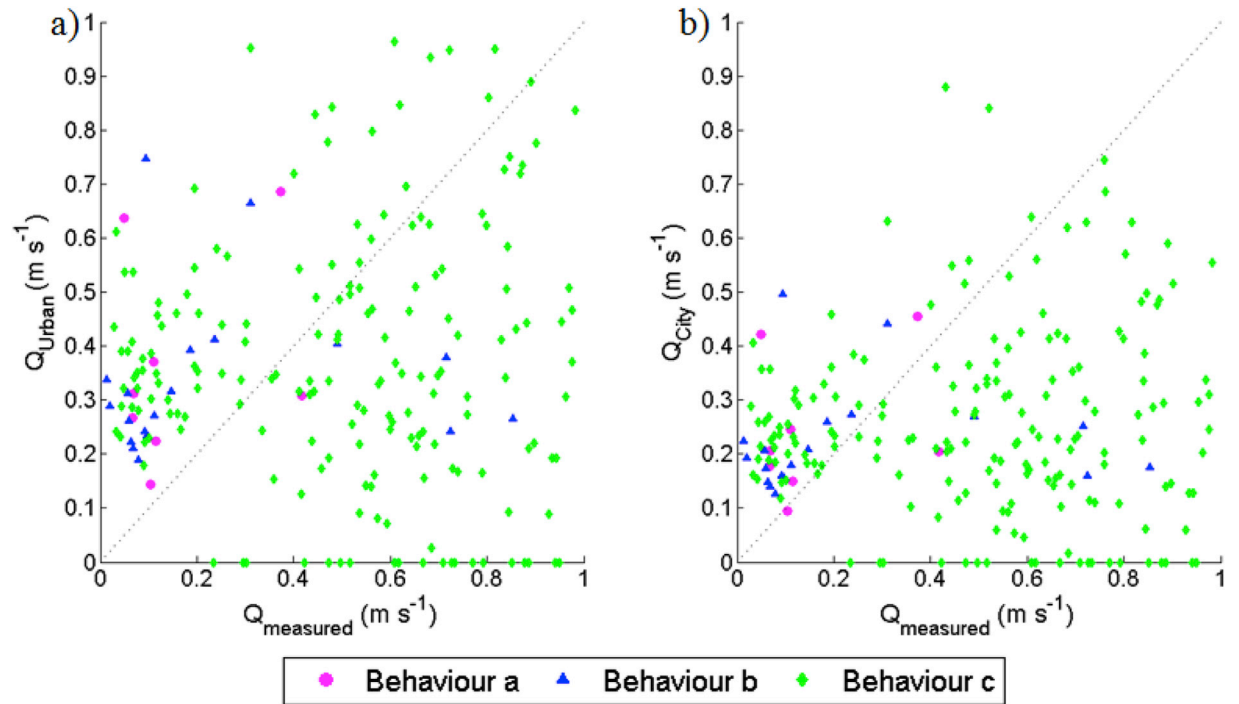


Fig. 9. Comparison of the RCC measured cross ventilation (Q_{measured}) and CIBSE wind speed model (Eq. (2)) with different coefficients (Table 2) a) Q_{Urban} , and b) Q_{City} (Fig. 6) for $\theta_{\text{ref}} = -45^\circ$ – 45° colour coded by behaviour as Fig. 8. Dashed line is a 1:1 line. (For interpretation of the references to colour in this figure legend, the reader is referred to the Web version of this article.)

difference in Q_N between the behaviours at $\theta_{\text{ref}} = 0^\circ$ is between ~ -0.1 to 1.4 (Fig. 8). There is little difference in Q_N for all other wind angles as the behaviours occur when the wind is perpendicular or nearly perpendicular to the instrumented cube (Fig. 8). This suggests that using predicted CIBSE wind speeds (Urban and City coefficients) to estimate the surface pressure will over-predict ventilation rates as behaviour c is not captured.

4. Comparing predicted ventilation rate to measured ventilation rate

For cross ventilation, pressure due to the wind (p_w) can be calculated:

$$p_w = 0.5 \rho C_p U^2 \quad (4)$$

where C_p is the pressure coefficient and U is a wind speed representative of the flow close to the building, in this case the predicted U_{local} . The pressure difference (Δp) in Eq. (1) can be defined as the difference between the windward (ww) and leeward (lw) face averaged pressures:

$$\Delta p = 0.5 \rho U_{local}^2 (C_{p,ww} - C_{p,lw}) \quad (5)$$

Leading to:

$$Q = C_d A \sqrt{U_{local}^2 (C_{p,ww} - C_{p,lw})} \quad (6)$$

When the CIBSE U_{local} with urban coefficients (Eq. (2)) is used to predict the RCC ventilation rates, they are overestimated compared to those measured for the array case (not shown). However, with limited data when $\theta_{ref} = -45^\circ$ – 45° , there are few behaviour a cases (Fig. 9). For behaviour b conditions ‘city’ coefficients provide an estimate that are closer to the measured values for low ventilation rates ($< 0.2 \text{ m}^3 \text{ s}^{-1}$) than the urban coefficients. However, it does not capture some of the higher ventilation rates which may be caused by a slight shift in θ_{ref} over the averaging period. The ventilation rates linked to behaviour c wind speed behaviours are not well predicted by either coefficient, as expected from Fig. 6, because of the direction effects and variation in the flow field around the instrumented cube are unaccounted for in Eq. (2). There is no clear relation between the predicted and measured ventilation rates (Fig. 9).

5. Discussion

The simplified full-scale staggered array in the RCC study, is informative as there are little full-scale data to which pressure measurements can be compared. Comparisons to the available sheltered models (CIBSE, 1997, 2006) suggest that the asymmetrical effects were not captured but the values are of the same order of magnitude (Gough, 2017). Comparison to previous isolated Silsoe cube pressure experiments (e.g. Straw et al., 2000; Richards and Hoxey, 2012) are also possible. When the isolated Silsoe cube had 1 m^2 openings, for the 90° wind direction, the pressure difference ventilation rates were 21% of the tracer gas decay results, as the opening size caused flow to be rapidly flushed from the cube (Straw et al., 2000).

Shortcomings of measuring ventilation rates by pressure difference have been highlighted by Demmers et al. (2001) and Samer et al. (2011). Comparison of the RCC pressure-based to tracer gas decay ventilation rates found poor agreement with a large degree of scatter rather than systematic bias (Gough et al., in review). It is improved for wind directions when openings lie within the cube wake, or when the cube is located within the array rather than isolated. The Gough et al. (in review) comparison included careful definition of errors based on sensor location, instrumental error and averaging time. The approach taken here, of using many measurements for a given wind direction, is justified given the inherent uncertainty in the pressure method. Further work to investigate the scatter in ventilation estimates includes assessing unsteadiness in both internal and external flow due to the full-scale meteorological conditions, including the ‘flow switching’ behaviour demonstrated here.

The deviation of the ventilation rate of an isolated cube from being symmetrical with wind direction appears to be caused by the sewage tanks ($\theta_{ref} = -90^\circ$ to -120°) and the storage shed ($\theta_{ref} = 70^\circ$ – 100°) (Fig. 1). When $\theta_{ref} = 90^\circ$ the front face pressure distribution was similar for the shed and no shed cases (as the flow is parallel) undertaken within the wind tunnel (1:200 model, in preparation) and in CFD models (King et al. 2017a,b), with the largest reduction in pressure coefficient (0.3) being on the North face. For the array case, the asymmetry of the array is the more dominant effect on the ventilation rate and pressure coefficients, with the influence of the tanks and shed being less. Ventilation rates are dependent on both buoyancy effects and wind-driven processes. Here, the focus is on wind-driven effects. Flow behaviours in the array are

likely to become more complex when surrounding buildings are heated (Kolokotroni et al., 2012).

Measurement campaigns within an urban area focusing on both surrounding flow patterns and pressure coefficient measurements are rare due to restrictions on sensor placement and difficulty in interpretation the data. Thermal measurement campaigns are more commonly undertaken in the urban area (e.g. Mavrogiani et al., 2011). The lack of accessible, usable and available weather data caused by differing research objectives for cities (in particular London) has been highlighted by Grimmond (2013). This lack of measurements within the urban area means that natural ventilation is designed using model data, such as the Design Summer years, the Test Reference Year for temperature by CIBSE (Short et al., 2004) and the London Heathrow dataset. This however may under predict the urban heat island effect and overestimate the wind speeds, due to Eq. (2) not explicitly including roughness lengths of the local surroundings. The data discussed here highlights that for a simplified, limited array of cubes within an urban area, the local wind speed to the test building is overestimated. Clear guidance is required about the geographical region for which each Design Summer Year and various wind speed models should be used, as the choice can have significant design and energy use consequences (Short et al., 2004).

6. Conclusions

The specific focus of this paper was to explore the impact of the array on the i) relation between local and reference wind speeds as modified by wind direction and ii) cross ventilation rates. The RCC full-scale data-set encompasses a much wider range of atmospheric conditions than previous studies, hence this paper presents an important contribution to addressing the effects of surrounding buildings on ventilation rate. Results have been reported for a 25.7% packing density full-scale staggered array which extends for three rows.

During the nine months RCC field campaign, a wide range of normalised cross ventilation rates occurred (Fig. 3, Table 1). For the isolated cube, maximum Q_N occurs, as expected, during perpendicular winds ($\theta_{ref} = 0^\circ$) with the minimum occurring for parallel cases ($\theta_{ref} = 90^\circ$). A range in Q_N of 0.2 or more is measured for all θ_{ref} directions. Asymmetry is caused by the effects of the storage shed and other site features for the isolated cube, though the asymmetry of the array masks the location based asymmetries (Figs. 1 and 7).

The array causes a 50%–90% reduction in ventilation rate when $\theta_{ref} = 0^\circ$ and the percentage decreases caused by the array varies with reference wind direction (Fig. 7). This is within the ranges predicted by CIBSE (2006) and van Hooff and Blocken (2010), 33% and 96% respectively. The limited nature of the RCC array causes little difference in ventilation rate for $\theta_{ref} = 180^\circ$ as the back face of the instrumented cube still being exposed on the edge of the array. This is also true for $\theta_{ref} = 90^\circ$ where the flow is parallel for both the isolated and array cases. Trends in the ventilation rate measurements for $\theta_{ref} = 0^\circ \pm 45^\circ$ can be linked to the variations in local wind behaviour.

It is concluded that use of wind speed based ventilation estimates within an urban area without a local wind speed measurement are subject to errors. This is because of the complex behaviour of the local flow within even a simple staggered array (Fig. 6). CIBSE methods which account for the effect of surroundings on the wind speed do not capture the split windspeed behaviour observed, which may lead to errors in ventilation rate estimates. The spatial scale upon which the flow varies within the array between wake and channelled regimes needs to be quantified, as nearby points may experience very different flow behaviours. However, these differences do not appear to have a great effect on pressure-based ventilation rates, possibly because the flow behaviour directly in front of the front cube face is different to that measured at the local mast (Figs. 1 and 8).

The three different behaviours observed between local and reference wind speeds were linked to channelling, wakes and wake reflections. As locations within an array are likely to experience different flow

behaviours, a simple parameter to account for the sheltering effect is insufficient. These results suggest that a simple flow model based on wake and channelling flows could be developed, similar to Dobre et al. (2005). In the future CFD data (e.g. King et al., 2017a, b) could be used to explore to determine if the split behaviour is captured within numerical flow models and if so where it is likely to occur within an array.

Although the mechanisms behind the split behaviour are not yet fully understood, these results suggest that simply treating flow in an urban area as a reduction in wind speeds will lead to inaccurate ventilation rates for some of the time (Fig. 9). This effect is hypothesized to vary for each location as a function of packing density and geometric details. Beyond wind speed, local wind direction needs to be considered concurrently as flow may be reversed compared to the reference flow (Fig. 4). Although of limited extent, it is likely that this behaviour will be observed for other layouts where the array elements are close enough to interact.

Acknowledgements

This work was funded by the EPSRC REFRESH (EP/K021893/1) project (<http://www.refresh-project.org.uk/>). Thanks to Solutions for Research and John Lally for assistance with the full-scale observations. Support from EPSRC LoHCool (EP/N009797/1) is also acknowledged. Datasets can be found at DOI: <https://doi.org/10.17864/1947.137>

Appendix A. Supplementary data

Supplementary data related to this article can be found at <https://doi.org/10.1016/j.jweia.2018.02.010>.

References

- Allocca, C., Chen, Q., Glicksman, L.R., 2003. Design analysis of single-sided natural ventilation. *Energy Build.* 35, 785–795. [https://doi.org/10.1016/S0378-7788\(02\)00239-6](https://doi.org/10.1016/S0378-7788(02)00239-6).
- Bakó-Biró, Z., Clements-Croome, D., 2012. Ventilation rates in schools and pupils' performance. *Build. Environ.* 48, 215–223. <https://doi.org/10.1016/j.buildenv.2011.08.018>.
- Barlow, J., Coceal, O., 2009. A Review of Urban Roughness Sublayer Turbulence: U.K Met Office Technical Report No. 527, Met Office Research and Development. Reading.
- Barlow, J.F., Halios, C.H., Lane, S.E., Wood, C.R., 2014. Observations of urban boundary layer structure during a strong urban heat island event. *Environ. Fluid Mech.* 15, 373–398. <https://doi.org/10.1007/s10652-014-9335-6>.
- Blocken, B., 2014. 50 years of computational wind engineering: past, present and future. *J. Wind Eng. Ind. Aerod.* 129, 69–102. <https://doi.org/10.1016/j.jweia.2014.03.008>.
- Boddy, J.W.D., Smalley, R.J., Dixon, N.S., Tate, J.E., Tomlin, A.S., 2005. The spatial variability in concentrations of a traffic-related pollutant in two street canyons in York, UK - Part I: the influence of background winds. *Atmos. Environ.* 39, 3147–3161. <https://doi.org/10.1016/j.atmosenv.2005.01.043>.
- Cheng, H., Hayden, P., Robins, A., Castro, I., 2007. Flow over cube arrays of different packing densities. *J. Wind Eng. Ind. Aerod.* 95, 715–740. <https://doi.org/10.1016/j.jweia.2007.01.004>.
- Cheng, V., Ng, E., Chan, C., Givoni, B., 2012. Outdoor thermal comfort study in a sub-tropical climate: a longitudinal study based in Hong Kong. *Int. J. Biometeorol.* 56, 43–56. <https://doi.org/10.1007/s00484-010-0396-z>.
- Choinière, Y., Tanaka, H., Munroe, J.A., Suchorski-Tremblay, A., 1992. Prediction of wind-induced ventilation for livestock housing. *J. Wind Eng. Ind. Aerod.* 44, 2563–2574. [https://doi.org/10.1016/0167-6105\(92\)90048-F](https://doi.org/10.1016/0167-6105(92)90048-F).
- CIBSE (Chartered Institute of Building Services Engineers), 2006. Guide a- Environmental Design. London.
- CIBSE, The Chartered Institution of Building Services Engineers, 1997. Natural Ventilation in Non-domestic Buildings, Applications Manual AM10.
- Coceal, O., Dobre, a., Thomas, T.G., Belcher, S.E., 2007. Structure of turbulent flow over regular arrays of cubical roughness. *J. Fluid Mech.* 589, 375–409. <https://doi.org/10.1017/S002211200700794X>.
- Demmers, T.G.M., Phillips, V.R., Short, L.S., Burgess, L.R., Hoxey, R.P., Wathes, C.M., 2001. Validation of ventilation rate measurement methods and the ammonia emission from naturally ventilated dairy and beef buildings in the United Kingdom. *J. Agric. Eng. Res.* 79, 107–116. <https://doi.org/10.1006/jaer.2000.0678>.
- Dobre, a., Arnold, S., Smalley, R., Boddy, J., Barlow, J., Tomlin, a., Belcher, S., 2005. Flow field measurements in the proximity of an urban intersection in London, UK. *Atmos. Environ.* 39, 4647–4657. <https://doi.org/10.1016/j.atmosenv.2005.04.015>.
- Gailis, R.M., Hill, A., 2006. A wind-tunnel simulation of plume dispersion within a large array of obstacles. *Boundary-Layer Meteorol.* 119, 289–338. <https://doi.org/10.1007/s10546-005-9029-1>.
- Gilleson, C.A., Camargo-Valero, M.A., Pickin, L.E., Noakes, C.J., 2013. Measurement of ventilation and airborne infection risk in large naturally ventilated hospital wards. *Build. Environ.* 65, 35–48. <https://doi.org/10.1016/j.buildenv.2013.03.006>.
- Gough, H., 2017. Effects of Meteorological Conditions on Building Natural Ventilation in Idealised Urban Settings. PhD thesis. University of Reading, Department of Meteorology.
- Grimmond, C.S.B., 2013. Observing London: Weather Data Needed for London to Thrive, London Climate Change Partnership Executive Summary. London.
- Grimmond, C.S.B., Blackett, M., Best, M.J., Barlow, J., Baik, J.J., Belcher, S.E., Bohnenstengel, S.L., Calmet, I., Chen, F., Dandou, A., Fortuniak, K., Gouvea, M.L., Hamdi, R., Hendry, M., Kawai, T., Kawamoto, Y., Kondo, H., Krayenhoff, E.S., Lee, S.H., Loridan, T., Martilli, A., Masson, V., Miao, S., Oleson, K., Pigeon, G., Porson, A., Ryu, Y.H., Salamanca, F., Shashua-Bar, L., Steeneveld, G.J., Tombrou, M., Voogt, J., Young, D., Zhang, N., 2010. The international urban energy balance models comparison project: first results from phase 1. *J. Appl. Meteorol. Climatol.* 49, 1268–1292. <https://doi.org/10.1175/2010JAMC2354.1>.
- Hall, D.J., Spanton, A.M., 2012. ADMLC Report 7 Annex a: Ingress of External Contaminants into Buildings – a Review. London.
- Hens, H., Sanders, C., Kumaran, M.K., Hagetoft, C.E., 1996. Heat, Air and Moisture Transfer through New and Retrofitted Insulated Envelope Parts (Hamtie): IEA Annex 24, first ed. Laboratorium Bouwfysica, Department Burgerlijke Bouwkunde, Leuven.
- Hummelgaard, J., Juhl, P., Sæbjørnsson, K.O., Clausen, G., Toftum, J., Langkilde, G., 2007. Indoor air quality and occupant satisfaction in five mechanically and four naturally ventilated open-plan office buildings. *Build. Environ.* 42, 4051–4058. <https://doi.org/10.1016/j.buildenv.2006.07.042>.
- Inagaki, A., Castillo, M.C.L., Yamashita, Y., Kanda, M., Takimoto, H., 2012. Large-Eddy simulation of coherent flow structures within a cubical canopy. *Boundary-Layer Meteorol.* 142, 207–222. <https://doi.org/10.1007/s10546-011-9671-8>.
- Inagaki, A., Kanda, M., 2010. Organized structure of active turbulence over an array of cubes within the logarithmic layer of atmospheric flow. *Boundary-Layer Meteorol.* 135, 209–228.
- Jiang, Y., Chen, Q., 2002. Effect of fluctuating wind direction on cross natural ventilation in buildings from large eddy simulation. *Build. Environ.* 37, 379–386.
- Kaimal, J.C., Finnigan, J.J., 1993. Atmospheric Boundary Layer Flows: Their Structure and Measurement: Their Structure and Measurement. Oxford University Press.
- Kanda, M., 2007. Progress in urban meteorology: a review. *J. Meteorol. Soc. Japan* 85B, 363–383. <https://doi.org/10.2151/jmsj.85B.363>.
- Karava, P., Stathopoulos, T., Athienitis, A. K., 2011. Airflow assessment in cross-ventilated buildings with operable façade elements. *Build. Environ.* 46, 266–279. <https://doi.org/10.1016/j.buildenv.2010.07.022>.
- King, M.-F., Gough, H.L., Halios, C., Barlow, J.F., Robertson, A., Hoxey, R., Noakes, C.J., 2017a. Investigating the influence of neighbouring structures on natural ventilation potential of a full-scale cubical building using time-dependent CFD (accepted). *J. Wind Eng. Ind. Aerod.* 169, 265–279. <https://doi.org/10.1016/j.jweia.2017.07.020>.
- King, M.-F., Khan, A., Delbosc, N., Gough, H.L., Halios, C., Barlow, J.F., Noakes, C.J., 2017b. Modelling urban airflow and natural ventilation using a GPU-based lattice-Boltzmann method. *Build. Environ.* 125, 273–284. <https://doi.org/10.1016/j.buildenv.2017.08.048>.
- Kolokotroni, M., Ren, X., Davies, M., Mavrogiani, A., 2012. London's urban heat island: impact on current and future energy consumption in office buildings. *Energy Build.* 47, 302–311. <https://doi.org/10.1016/j.enbuild.2011.12.019>.
- Kolokotroni, M., Tassou, S.A., Gowreesunker, B.L., 2015. Energy aspects and ventilation of food retail buildings. *Adv. Build. Energy Res.* 9, 1–19. <https://doi.org/10.1080/17512549.2014.897252>.
- Liddament, M., 1996. A Guide to Energy Efficient Ventilation. Coventry U.K.
- Macdonald, R., Griffiths, R., Hall, D., 1998. A comparison of results from scaled field and wind tunnel modelling of dispersion in arrays of obstacles. *Atmos. Environ.* 32, 3845–3862.
- Mavrogiani, A., Davies, M., Batty, M., Belcher, S.E., Bohnenstengel, S.L., Carruthers, D., Chalabi, Z., Croxford, B., Demanuele, C., Evans, S., Giridharan, R., Hacker, J.N., Hamilton, I., Hogg, C., Hunt, J., Kolokotroni, M., Martin, C., Milner, J., Rajapaksha, I., Ridley, I., Steadman, J.P., Stocker, J., Wilkinson, P., Ye, Z., 2011. The comfort, energy and health implications of London's urban heat island. *Build. Serv. Eng. Technol.* 32, 35–52. <https://doi.org/10.1177/0143624410394530>.
- Nelson, M.A., Pardyjak, E.R., Klewicki, J.C., Pol, S.U., Brown, M.J., 2007. Properties of the wind field within the Oklahoma city park avenue street canyon. Part I: mean flow and turbulence statistics. *J. Appl. Meteorol. Climatol.* 46, 2038–2054. <https://doi.org/10.1175/2006JAMC1427.1>.
- Ogink, N.W.M., Mosquera, J., Calvet, S., Zhang, G., 2013. Methods for measuring gas emissions from naturally ventilated livestock buildings: developments over the last decade and perspectives for improvement. *Biosyst. Eng.* 116, 297–308. <https://doi.org/10.1016/j.biosystemseng.2012.10.005>.
- Richards, P., Hoxey, R., 2007. Wind-tunnel modelling of the Silsoe cube. *J. Wind Eng. Ind. Aerod.* 95, 1384–1399. <https://doi.org/10.1016/j.jweia.2007.02.005>.
- Richards, P., Hoxey, R., Short, L., 2001. Wind pressures on a 6m cube. *J. Wind Eng. Ind. Aerod.* 89, 1553–1564.
- Richards, P.J., Hoxey, R.P., 2012a. Pressures on a cubic building-Part 2: quasi-steady and other processes. *J. Wind Eng. Ind. Aerod.* 102, 87–96. <https://doi.org/10.1016/j.jweia.2011.11.003>.
- Richards, P.J., Hoxey, R.P., 2012b. Pressures on a cubic building—Part 1: full-scale results. *J. Wind Eng. Ind. Aerod.* 102, 72–86. <https://doi.org/10.1016/j.jweia.2011.11.004>.

- Richards, P.J., Hoxey, R.P., 2008. Wind loads on the roof of a 6m cube. *J. Wind Eng. Ind. Aerod.* 96, 984–993. <https://doi.org/10.1016/j.jweia.2007.06.032>.
- Richards, P.J., Hoxey, R.P., 2002. Unsteady flow on the sides of a 6m cube. *J. Wind Eng. Ind. Aerod.* 90, 1855–1866. [https://doi.org/10.1016/S0167-6105\(02\)00293-3](https://doi.org/10.1016/S0167-6105(02)00293-3).
- Samer, M., Berg, W., Muller, H.-J., Fiedler, M., Glaser, M., Ammon, C., Sanftleben, P., Brunsch, R., 2011. Radioactive ⁸⁵Kr and CO₂ balance for ventilation rate measurements and gaseous emissions quantification through naturally ventilated barns. *Trans. ASABE (Am. Soc. Agric. Biol. Eng.)* 54, 1137–1148. <https://doi.org/10.13031/2013.37105>.
- Santamouris, M., Papanikolaou, N., Livada, I., Koronakis, I., Georgakis, C., Argiriou, a, Assimakopoulos, D., 2001. On the impact of urban climate on the energy consumption of buildings. *Sol. Energy* 70, 201–216. [https://doi.org/10.1016/S0038-092X\(00\)00095-5](https://doi.org/10.1016/S0038-092X(00)00095-5).
- Sato, A., Michioka, T., Takimoto, H., Kanda, M., 2010. Field and wind tunnel experiments about flow and dispersion within street canyons. In: *Proceedings of the Fifth International Symposium on Computational Wind Engineering (CWE2010)*, Chapel Hill, NC, USA.
- Short, C.A., Lomas, K.J., Woods, A., 2004. Design strategy for low-energy ventilation and cooling within an urban heat island. *Build. Res. Inf.* 32, 187–206. <https://doi.org/10.1080/09613210410001679875>.
- Straw, M., 2000. *Computation and Measurement of Wind Induced Ventilation*. PhD thesis. University of Nottingham.
- Straw, M., Baker, C., Robertson, A., 2000. Experimental measurements and computations of the wind-induced ventilation of a cubic structure. *J. Wind Eng. Ind. Aerod.* 88, 213–230. [https://doi.org/10.1016/S0167-6105\(00\)00050-7](https://doi.org/10.1016/S0167-6105(00)00050-7).
- van Hooff, T., Blocken, B., 2010. On the effect of wind direction and urban surroundings on natural ventilation of a large semi-enclosed stadium. *Comput. Fluids* 39, 1146–1155. <https://doi.org/10.1016/j.compfluid.2010.02.004>.
- Wilczak, J.M., Oncley, S.P., Stage, S.A., 2001. Sonic Anemometer Tilt Correction Algorithms, pp. 127–150.
- Wood, C.R., Lacser, A., Barlow, J.F., Padhra, A., Belcher, S.E., Nemitz, E., Helfter, C., Famulari, D., Grimmond, C.S.B., 2010. Turbulent flow at 190 m height above London during 2006–2008: a climatology and the applicability of similarity theory. *Boundary-Layer Meteorol.* 137, 77–96.
- Yang, T., Wright, N., Etheridge, D., Quinn, A., 2006. A comparison of CFD and full-scale measurements for analysis of natural ventilation. *Int. J. Vent.* 4, 337–348.
- Yuan, C., Ng, E., 2012. Building porosity for better urban ventilation in high-density cities – a computational parametric study. *Build. Environ.* 50, 176–189. <https://doi.org/10.1016/j.buildenv.2011.10.023>.
- Zaki, S., Hagishima, A., Tanimoto, J., Ikegaya, N., 2010. Wind tunnel measurement of aerodynamic parameters of urban building arrays with random geometries. In: *Proceedings of the Fifth International Symposium on Computational Wind Engineering (CWE2010)*, Chapel Hill, NC, USA.